

## Dependence of ion-electron emission from clean metals on the incidence angle of the projectile

J. Ferrón, E. V. Alonso, R. A. Baragiola, and A. Oliva-Florio\*

*Centro Atómico Bariloche, Comisión Nacional de Energía Atómica,  
Instituto Balseiro, Universidad Nacional de Cuyo, 8400 Bariloche, Argentina*

(Received 9 February 1981)

We have studied the dependence of electron yields  $\gamma$  from clean Cu and Au surfaces on the incidence angle  $\theta$  of 5–50-keV He<sup>+</sup>, Ar<sup>+</sup>, and Xe<sup>+</sup> projectiles, in the angular range 0°–80°, and under ultrahigh-vacuum conditions. We have found that, at small angles,  $\gamma \propto \sec^f \theta$ , with  $f$  generally different from unity. For Xe<sup>+</sup> on Cu,  $\gamma(\theta)$  presents an energy-dependent maximum, similar to that obtained for sputtering. The results are explained in terms of the anisotropy of the electron cascade in the solid, and the depth distribution of the inelastic energy deposited by the projectile, and by rapidly recoiling target atoms in the near-surface region of the solid.

## I. INTRODUCTION

When the surface of a solid body is bombarded by ions, electron emission (EE) may be observed. A measure of this phenomenon is the total EE yield  $\gamma$ , defined as the average number of electrons emitted per incident ion. It is formally possible to distinguish two different mechanisms for EE depending on whether the main source of energy required to liberate electrons from the target is given by the neutralization energy of the incident ion or by its kinetic energy. The former is known as potential EE (PEE) and, being exothermic, it can occur even at zero kinetic energy. The latter mechanism is known as kinetic electron emission (KEE) and predominates above a certain threshold of  $(0.4-2) \times 10^7$  cm/s for clean surfaces. PEE has been studied in detail by Hagstrum<sup>1</sup> and it is fairly well understood in terms of an Auger transition involving two electrons from the valence band of the solid and the hole in the incoming ion. In KEE it has been argued in the past that the main electron-excitation process is the Auger decay of inner-shell excited target atoms<sup>2</sup> or the direct ionization of the projectile.<sup>3</sup> Recently we have shown that, at least in the energy range from threshold to a few tens of keV, excitation of target valence-band electrons by the projectile is the dominant process in KEE.<sup>4-6</sup>

Most of the previous work on EE by ions on clean metals has been performed for normal incidence of the ion beam on the target surface: However, a few exceptions exist,<sup>7</sup> particularly on single-crystal targets<sup>8</sup> where the effect of the incidence angle of the projectiles was studied. Analysis of data of  $\gamma(\theta)$  obtained over a wide range

of energies and projectile-target mass ratios can potentially lead to more information on basic phenomena by emphasizing aspects of the atomic and electronic collision cascades created in the solid by the projectile.

In this paper we present measurements of  $\gamma(\theta)$  dependences for Cu and Au bombarded by He<sup>+</sup>, Ar<sup>+</sup>, and Xe<sup>+</sup> projectiles in the energy range 5–50 keV, in the angular range 0°–80°, and under ultrahigh-vacuum conditions. We discuss the results taking into account the anisotropy of the electron cascade in the solid, and the depth distribution of electronic excitations produced by the projectile and recoiling target atoms.

## II. EXPERIMENTAL DETAILS

The basic equipment has been described in detail previously<sup>4</sup> so we will limit ourselves here to a brief description, stressing the differences in the new target-collector system which was built to allow for oblique incidence of the ion beam. A conventional accelerator equipped with a radio-frequency ion source is used to produce the ion beam, which, after mass analysis, passes through collimators into a differential pumping chamber kept at  $\sim 10^{-8}$  Torr and then into the target chamber which is kept at  $\sim 10^{-10}$  Torr during measurements. The beam energy is known to within  $\pm(0.1\% + 30 \text{ eV})$  and the fraction of neutrals in the beam, produced by electron capture from residual gas molecules and collimating slits, is in all cases below 2%. To evaluate the influence of excited ions in the beam which may be produced in the ion source, and survive the transit to the target, we have varied the operating condi-

tions in the source (which should have altered the proportion of excited ions in the beam), but found no effect within our statistical errors of  $\pm 3\%$ .

The measurement device is shown in Fig. 1. The target is biased at  $V_t = -30$  V and the collector at  $V_c = 80$  V with respect to ground. These voltages are larger than those required to reach saturation in the measured currents. A suppressor electrode, biased at  $V_s = -200$  V, prevents electrons from escaping the collector and also prevents electrons external to the target-collector system from entering this region. A shielding electrode, biased at the same voltage as the suppressor, serves mainly to suppress electrons coming from the ion pump. The shielding and the collector have holes which are used for optical alignment and to allow deposition of fresh metal layers onto the sample from an evaporation source located below it. The presence of these holes does not affect the measurements, as deduced from the fact that the results did not depend on the sign of rotation of the target, i.e.,  $\gamma(\theta) = \gamma(-\theta)$ . The target is mounted in a goniometer, and the positions  $0^\circ$ ,  $90^\circ$ , and  $-90^\circ$  were determined with an uncertainty of  $0.1^\circ$ .

The current measured at the collector is composed of electrons from the target and reflected and sputtered ions. In a previous work<sup>4</sup> we found that for normal incidence of the beam, the secondary ion emission amounted to less than 4%, our total experimental uncertainty. In the present work, another study was required since both projectile reflection and sputtering increase with angle of incidence. To evaluate this effect, we placed a magnetic field parallel to the axis of rotation of the sample, which could be varied between 0 and 200 Oe. With the

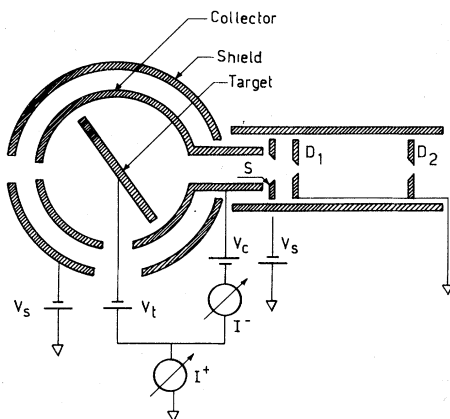


FIG. 1. Schematic drawing of the collimators and the target collector assembly.  $D_1$  and  $D_2$  are the collimators, and S the electron suppressor.

higher field and our geometry, essentially all electrons are returned to the target (or to the collector if they are produced there by secondary ions), since only electrons of energy larger than about 3 keV can escape the influence of the magnetic field and reach another electrode. In this way, we determined that in all cases, and even for incidence angles of  $80^\circ$ , the number of secondary ions (whose trajectories are not appreciably affected by magnetic fields of the magnitude used) was less than 1% of the electron current, in essential agreement with the work of Evdokimov *et al.*<sup>7</sup>

A correction was needed to the measurements of the angle of incidence  $\theta$ , particularly at large  $\theta$  and small ion energies, due to the deflection of the ion beam by the electric field between target and collector. These corrections were determined in sputtering experiments<sup>9</sup> and were of  $3^\circ$  for 10-keV ions and  $0.6^\circ$  for 50-keV ions, both at  $\theta = 80^\circ$ . The data to be presented below is corrected for this effect. The total uncertainties in the measurements of incidence angles are  $\pm 0.3^\circ$ .

The target preparation was analogous to that described before.<sup>4</sup> The targets were produced by evaporation of high purity (better than 99.999%) metals at pressures which were kept at  $\sim 10^{-9}$  Torr during deposition and decreased in a few seconds to

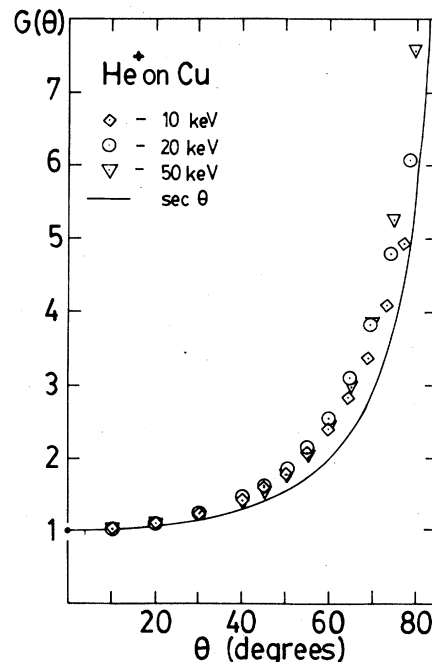


FIG. 2. Normalized KEE yields for  $\text{He}^+$  on Cu versus the angle of incidence. The PEE yield used is 0.24 (Ref. 10).

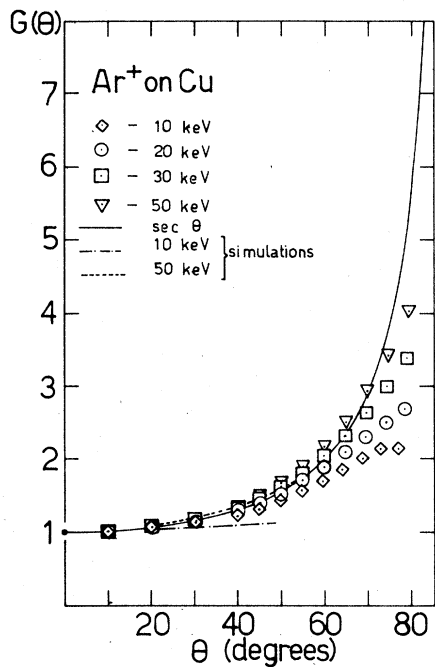


FIG. 3. Normalized KEE yields for  $\text{Ar}^+$  on Cu versus the angle of incidence. The PEE yield used is 0.08 (Ref. 10). Also shown are the results of the Monte Carlo simulations described in the text, with isotropic sources.

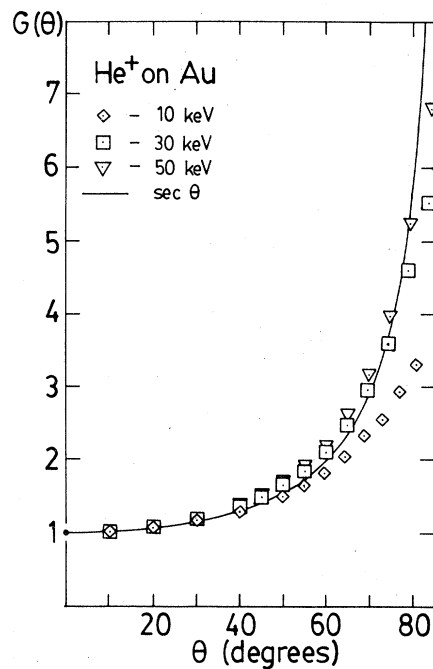


FIG. 5. Normalized KEE yields for  $\text{He}^+$  on Au versus the angle of incidence. The PEE yield used is 0.19 (Ref. 10).

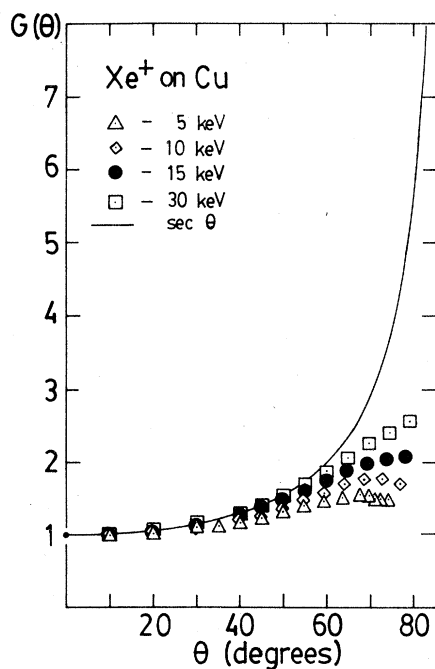


FIG. 4. Normalized KEE yields for  $\text{Xe}^+$  on Cu versus the angle of incidence. The PEE yield used is 0.02 (Ref. 10).

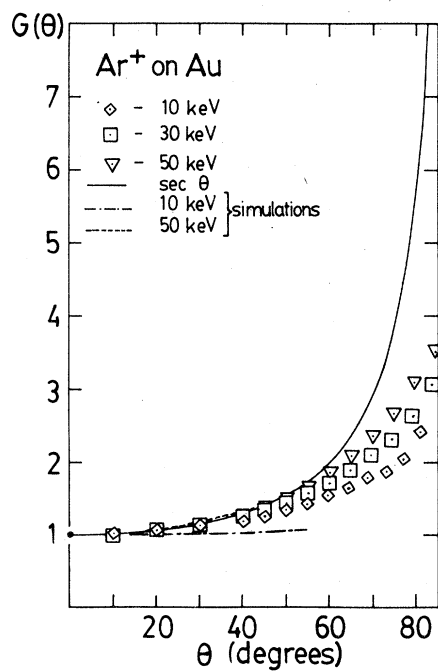


Fig. 6. Normalized KEE yields for  $\text{Ar}^+$  on Au versus the angle of incidence. The PEE yield used is 0.04 (Ref. 10). Also shown are the results of the Monte Carlo simulations described in the text, with isotropic sources.

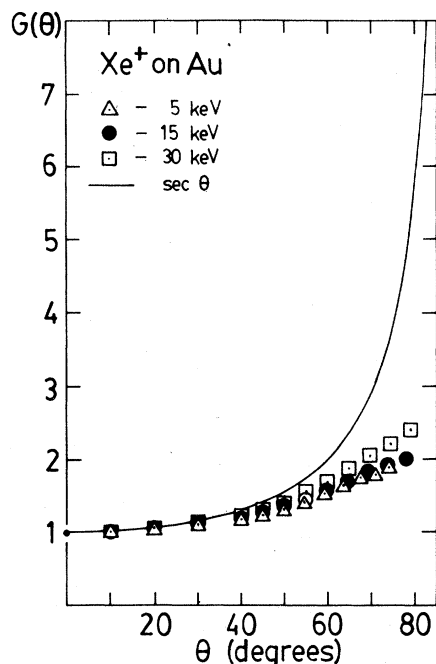


FIG. 7. Normalized KEE yields for  $\text{Xe}^+$  on Au versus the angle of incidence. The PEE yield was considered negligible (Ref. 10).

the  $10^{-10}$  Torr range upon completion of the evaporation.

### III. EXPERIMENTAL RESULTS

Our experimental results are presented in Figs. 2–7, normalized to the electron yields at normal incidence ( $\theta=0^\circ$ ) (Table I). Since we want to study KEE, we have subtracted in all cases the contribution of PEE  $\gamma_p$  using the formula of Kishinevskii,<sup>10</sup> which has been shown to agree very well with experiment.<sup>11</sup> We have assumed that  $\gamma_p$  does not depend on angle. Following the results of

Vance,<sup>12</sup> this should be a fairly good assumption. In any case, the influence of PEE amounts to less than 5% in all the cases studied.

One can observe that in many cases the function  $G(\theta) = \gamma_k(\theta)/\gamma_k(0)$ , with  $\gamma_k = \gamma - \gamma_p$ , grows faster than  $\sec\theta$  at small  $\theta$ , in discrepancy with previous reports.<sup>7,8</sup> For large angles  $G(\theta)$  falls below the  $\sec\theta$  curve, with  $\text{He}^+$  on Cu as the only exception, in essential agreement with the results of Evdokimov *et al.*<sup>7</sup> It was found that  $G(\theta)$  can be adjusted over a fairly large range of angles ( $\theta \leq 60^\circ$ ) with an expression  $G(\theta) = \sec^f\theta$ . The exponent  $f$  depends on energy and ion-target combination, increasing with increasing energy and decreasing with increasing mass of the projectile and/or target atoms (Table II). In the case of  $\text{Xe}^+$  on Su (Fig. 4),  $G(\theta)$  has a maximum at large incidence angles. The angle at which this maximum occurs is energy dependent, being greater the larger the energy. An embryonic maximum is also apparent in the data for 10-keV  $\text{Ar}^+$  on Cu (Fig. 3).

### IV. DISCUSSION

In the semiempirical model of KEE,<sup>4,5</sup> the yield is written as

$$\gamma = C \int_0^{x_n} N(R) e^{-x/L} dR, \quad (1)$$

where  $x$  is the coordinate normal to the surface,  $R$  the path traversed by the ion,  $N(R)$  the number of excited electrons produced in  $dR$  at  $R$ ,  $L$  the mean electron attenuation length,  $C$  a target-dependent constant, and  $x_n$  the distance at which the ion loses its capability to eject electrons. If the path of the ion is rectilinear ( $R = x \sec\theta$ ) and its electron excitation efficiency constant [ $N(R) = N$ ] over distances much larger than  $L$ , we can approximate the integral in Eq. (1) and get

TABLE I. Total electron emission yields  $\gamma(0)$  for normal incidence  $\text{He}^+$ ,  $\text{Ar}^+$ , and  $\text{Xe}^+$  ions on Cu and Au targets. Errors are  $\pm 5\%$ .

Target	Projectile	Energy (keV)					
		5	10	15	20	30	50
Cu	$\text{He}^+$		0.69		1.05		1.87
	$\text{Ar}^+$		0.91		1.54	2.15	2.82
	$\text{Xe}^+$	0.27	0.59	0.84		1.53	
Au	$\text{He}^+$		1.17			2.57	3.22
	$\text{Ar}^+$		0.39			1.36	2.26
	$\text{Xe}^+$	0.1		0.52		1.14	

TABLE II. Experimental  $f$  in  $\gamma(\theta) \propto \sec^f \theta$  for different energies and ion-target combinations. Errors are  $\pm 5\%$ .

Target	Projectile	Energy (keV)					
		5	10	15	20	30	50
Cu	He <sup>+</sup>		1.30		1.37		1.24
	Ar <sup>+</sup>		0.83		1.01	1.08	1.16
	Xe <sup>+</sup>	0.64	0.68	0.92		0.97	
Au	He <sup>+</sup>		0.89			1.13	1.20
	Ar <sup>+</sup>		0.65			0.80	1.00
	Xe <sup>+</sup>	0.57		0.67	0.77		

$$\gamma = CLN \sec \theta . \quad (2)$$

In the more general case, in which there is a variation of the number of excited electrons along the projectile path, one can derive, taking  $N(R) = N(0) + R(dN/dR)_{R=0}$  near the surface, the following approximation:

$$\gamma = CLN \sec^f \theta , \quad (3)$$

with

$$f = 1 + \frac{AL}{1 + AL} , \quad (4)$$

which is valid for small angles ( $\theta < 60^\circ$ ) and small  $A = [1/N(0)](dN/dR)_{R=0}$ , the normalized gradient of the density of excited electrons at the surface ( $|AL| < 1$ ). We will now discuss several factors that can be identified to cause an angular dependence weaker than  $\sec \theta$  ( $A < 0$ ), such as the shadowing of atomic planes<sup>7</sup> or the slowing down of the projectile, or for a stronger dependence than  $\sec \theta$  ( $A > 0$ ), such as the generation of excited electrons by recoiling target atoms, a nonrectilinear trajectory of the ion, and anisotropy in the source of excited electrons.

#### A. Scattering and slowing down of the projectile

The slower growth of  $G(\theta)$  compared with  $\sec \theta$  ( $A < 0$ ) for heavy projectiles has been observed previously. Evdokimov *et al.*<sup>7</sup> interpreted this effect with a "transparency" model based on the decrease in the probability of collision at large angles of incidence due to the shadowing of atomic planes lying near and below the surface by surface atoms. In contrast, Perdrix *et al.*<sup>13</sup> proposed that this effect is due to the slowing down of the projectile in the region of greater electron escape probability.

To study the effect of the slowing down and non-linear trajectory of the projectile in the target, we have used a Monte Carlo simulation<sup>14</sup> in which the collisions are described with the Molière approximation to the Thomas-Fermi interatomic potential. We calculated, using Firsov's friction model,<sup>15</sup> the inelastic energy deposited by the projectile in collisions with energy transfer larger than the work function of the target. We have adopted the value of 20 Å for  $L$ ,<sup>16</sup> the only material constant which does not disappear upon normalization to normal incidence, but we found that changes in  $L$  as large as 20% produced changes of only 5% in the calculated  $G(\theta)$ . Electronic excitation by fast recoiling target atoms (see below) was not considered in these calculations. We have found that only in the case of Ar<sup>+</sup> on Au, and for energies larger than 30 keV, the calculated  $G(\theta)$  grows faster than  $\sec \theta$  at small angles, but in all cases below the experimental data. The dominant effect is the slowing down of the projectile over distances of order  $L$ , which causes  $G(\theta)$  to grow slower than  $\sec \theta$ , the more so, the heavier and slower the ion, and the larger its angle of incidence.

#### B. Influence of recoiling target atoms

To study this effect we have modified the Monte Carlo simulation program to follow the trajectories of recoiling target atoms and the inelastic energy deposited by them. If we consider only EE caused by these recoils, the angular dependence is found in the majority of cases to grow faster than  $\sec \theta$ , due to the shape of the collision cascade. However, the relative influence of the recoils in practically all cases is so small that it does not affect substantially the functional shape of the total  $G(\theta)$ . In the case of 50-keV Ar<sup>+</sup> on Cu, EE produced by recoils causes

the calculated  $G(\theta)$  to grow faster than  $\sec\theta$ , but, nevertheless, below the experimental data (Fig. 3).

To estimate the importance of recoils in KEE Mashkova and Molchanov<sup>17</sup> performed comparative studies of angular dependences of KEE and sputtering, using 30-keV  $\text{Ar}^+$  ions on polycrystalline Cu, Ni, Mo, and W. They found that the maximum which is observed in all cases in the sputtering yield as a function of incidence angle did not appear in electron emission up to angles of  $86^\circ$ . The maximum in sputtering is due to the interruption in the development of the atomic collision cascade by the presence of the surface, since at large incidence angles many fast primary recoils can escape into vacuum depositing, on the average, a small amount of energy near the surface. For these reasons, and after not observing a maximum in their  $\gamma(\theta)$  curves, Mashkova and Molchanov concluded that recoiling atoms do not play an important role in KEE. For larger projectile-to-target mass ratios, as in the case of  $\text{Xe}^+$  on Cu used in this work, faster recoils, with more ability to excite electrons, are produced than in the case of  $\text{Ar}^+$  projectiles, and it is for this reason that the curves in Fig. 4 have maxima. One can also notice that the angle at which the maximum occurs  $\theta_m$  increases with increasing energy, showing the same dependence as that observed for sputtering. In Table III we present values of  $\theta_m$  obtained in this work, and compare them to those observed for sputtering in our laboratory.<sup>9</sup>

From the discussion above, one can conclude that the effect of nonrectilinear projectile motion and of KEE induced by fast recoils are not sufficient to account for the faster growth of  $G(\theta)$  compared with  $\sec\theta$ , as observed in some cases, whereas the maximum in  $G(\theta)$  for  $\text{Xe}^+$  on Cu can be explained as an effect due to electronic excitations by fast recoiling target atoms.

TABLE III. Values of  $\theta_m$ , the angle at which the maximum of electron emission and sputtering (Ref. 9) occur, for  $\text{Xe}^+$  on Cu.

Energy (keV)	$\theta_m$ for electron emission	$\theta_m$ for sputtering
5	$67^\circ$	$65^\circ$
10	$71^\circ$	$71^\circ$
30	$> 80^\circ$	$76^\circ$

### C. Anisotropy in the source of excited electrons

Electron emission in gas-phase collisions at not too large velocities is produced preferentially in the direction of motion of the projectile.<sup>18</sup> In a solid, excited electrons are also produced anisotropically,<sup>19,20</sup> but since the mean free paths for elastic and inelastic collisions are small<sup>16,21</sup> and since these collisions give nearly isotropic scattering at low electron energies, the anisotropy of the source tends to become obliterated. However, a residual anisotropy survives this process of isotropization and is responsible, for instance, for the greater electron emission in the direction of motion of the projectile than in the backward direction when thin solid films are bombarded by ions<sup>20,22,23</sup>.

The effect of this source anisotropy will be to transport electronic energy away from the entrance surface of the target and thus, recalling Eq. (3), to cause  $A > 0$  and  $f > 1$  in the initial growth law  $G(\theta) = \sec^f\theta$ . This effect has been earlier recognized by Sternglass<sup>19</sup> who was able to derive some simple estimates for  $N(R)$  in Eq. (1), for the case of high-velocity light ions.

Our experimental results show that, in general,  $f$  is larger the larger the energy of the projectile, and so they are consistent with those from gas-phase ionization collisions<sup>18</sup> where it is observed that anisotropy grows with projectile energy. We have also found that  $G(\theta)$  is greater for Cu than for Au for the same projectile and energy. In the case of He projectiles, where slowing down in distances of order  $L$  is unimportant, we can explain this effect in terms of a smaller residual anisotropy in Au because of its larger atomic potential and therefore its larger capability for isotropization.<sup>23</sup> For the heavier projectiles, alternative explanations based on differences in projectile scattering and stopping could at least partially account for these target dependences.

The anisotropy in the source is more pronounced for larger electron energies.<sup>20</sup> Fast electrons are also less likely to be randomized in their direction of motion by elastic collisions with ion cores. Therefore it seems reasonable to think that if we energy analyze the ejected electrons we will find that the anisotropy effect will be greater the larger their energy. In Fig. 8 we show the effect on  $G(\theta)$  of a magnetic field parallel to the axis of rotation of the target. This field prevents electrons of low energy from reaching the collector, and therefore it performs a crude energy analysis. It is observed that

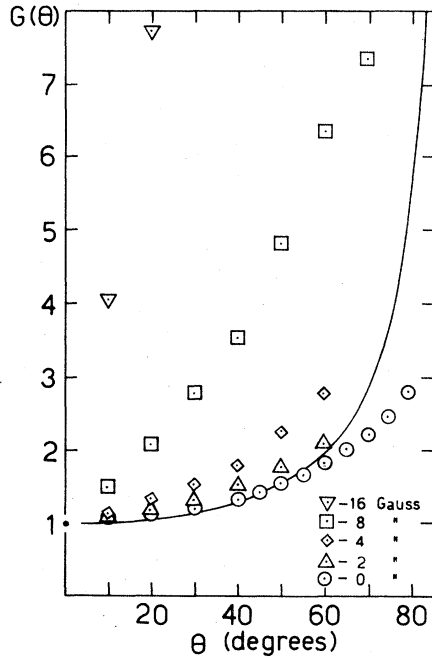


FIG. 8. Normalized KEE yields for 30-keV  $\text{Ar}^+$  on Au versus the angle of incidence, for different values of magnetic field applied parallel to the target surface and the axis of rotation.

the anisotropy effect, i.e., the growth of  $G(\theta)$  faster than  $\sec\theta$ , is more pronounced as the magnetic field (and therefore energy of the collected electrons) is increased. Other evidence for the anisotropy of the source has been provided by Begrambekov *et al.*<sup>24</sup>

for protons on Mo using a different experimental approach.

## CONCLUSIONS

We have found that, in general, the dependence of KEE with the incidence angle of the projectile deviates from the secant law. We have identified, as factors contributing to this behavior, the scattering and slowing down of the projectiles over distances of the order of the mean electron attenuation length, electron emission produced by fast recoiling target atoms, and anisotropy in the distribution of primary excited electrons in the solid. A conspicuous manifestation of KEE from fast recoils occurs for  $\text{Xe}^+$  on Cu, due to the large projectile-to-target mass ratio, where the  $\gamma(\theta)$  curves present an energy-dependent maximum at large angles, similar to the case of sputtering.

## ACKNOWLEDGMENTS

This work was partially supported by the International Atomic Energy Agency. We thank Mario Jakas for his help in the development of the computer simulation program, and to Jochen Biersack for making the TRIM code available to us before publication. We also thank Humberto Raiti, Jorge De Pellegrin, and Carlos Wenger for their help with the experiments.

\*Deceased.

<sup>1</sup>H. D. Hagstrum, *Phys. Rev.* **96**, 325 (1954).

<sup>2</sup>E. S. Parilis and L. M. Kishinevskii, *Fiz. Tverd. Tela (Leningrad)* **3**, 1219 (1960) [*Sov. Phys.—Solid State* **3**, 885 (1961)].

<sup>3</sup>D. E. Harrison, C. E. Carlston, and G. D. Magnuson, *Phys. Rev.* **139**, 3A (1965).

<sup>4</sup>R. A. Baragiola, E. V. Alonso, and A. Oliva-Florio, *Phys. Rev. B* **19**, 121 (1979).

<sup>5</sup>E. V. Alonso, R. A. Baragiola, J. Ferrón, M. M. Jakas, and A. Oliva-Florio, *Phys. Rev. B* **22**, 80 (1980).

<sup>6</sup>J. Ferrón, E. V. Alonso, R. A. Baragiola, and A. Oliva-Florio, *J. Phys. D* (in press).

<sup>7</sup>I. N. Evdokimov, E. S. Mashkova, V. A. Molchanov, and D. D. Odintsov, *Phys. Status Solidi* **19**, 407 (1967).

<sup>8</sup>N. Cook and R. B. Burt, *J. Phys. D* **8**, 812 (1975).

<sup>9</sup>A. Oliva-Florio, R. A. Baragiola, E. V. Alonso, and J. Ferrón (unpublished).

<sup>10</sup>L. M. Kishinevskii, *Radiat. Eff.* **19**, 23 (1973).

<sup>11</sup>H. Oeschner, *Phys. Rev. B* **17**, 1052 (1978); R. A. Baragiola, E. V. Alonso, J. Ferrón, and A. Oliva-Florio, *Surf. Sci.* **90**, 240 (1979).

<sup>12</sup>D. N. Vance, *Phys. Rev.* **169**, 2 (1968).

<sup>13</sup>M. Perdrix, S. Paletto, R. Goutte, and C. Guillaud, *J. Phys. D* **1**, 1517 (1968).

<sup>14</sup>J. Biersack and L. G. Haggmark, *Nucl. Instrum. Methods* **174**, 257 (1980); J. Biersack (private communication).

<sup>15</sup>O. B. Firsov, *Zh. Eksp. Teor. Fiz.* **36**, 1076 (1959) [*Sov. Phys.—JETP* **9**, 1076 (1959)]; L. M. Kishinevskii, *Izv. Akad. Nauk SSSR, Ser. Fiz.* **26**, 1410 (1962) [*Bull. Acad. Sci. USSR, Phys. Ser.* **26**, 1443 (1962)].

- <sup>16</sup>C. J. Tung, J. C. Ashley, and R. H. Ritchie, *Surf. Sci.* **81**, 427 (1980).
- <sup>17</sup>E. S. Mashkova and V. A. Molchanov, *Zh. Tekh. Fiz.* **34**, 2081 (1964) [*Sov. Phys.—Tech. Phys.* **9**, 1601 (1965)].
- <sup>18</sup>R. K. Cack and T. Jorgensen, Jr. *Phys. Rev. A* **4**, 1322 (1970); M. E. Rudd, *Radiat. Res.* **64**, 153 (1975).
- <sup>19</sup>E. J. Sternglass, *Phys. Rev.* **1**, 108 (1957).
- <sup>20</sup>W. Meckbach, G. Braunstein, and N. Arista, *J. Phys.* **B 8**, L344 (1975); W. Meckbach, in *Beam Foil Spectroscopy*, edited by I. A. Sellin and D. J. Pegg (Plenum, New York, 1975), Vol. 2, p. 577.
- <sup>21</sup>C. B. Duke, *Crit. Rev. Solid State Sci.* **4**, 125 (1974); J. B. Pendry, *Low Energy Electron Diffraction* (Academic, New York, 1974), Ch. 2.
- <sup>22</sup>E. S. Mironov and L. M. Nemenov, *Zh. Eksp. Teor. Fiz.* **30**, 269 (1957) [*Sov. Phys.—JETP* **5**, 188 (1957)]; J. N. Anno and R. G. Jung, *J. Appl. Phys.* **36**, 3949 (1965).
- <sup>23</sup>E. L. Haines, A. B. Whitehead, and R. A. Parker, in *Beam Foil Spectroscopy*, edited by S. Bashkin (Gordon and Breach, New York, 1968), p. 177.
- <sup>24</sup>L. B. Begrambekov, S. K. Zhdanov, and V. G. Telkovskii, *Fiz. Tverd. Tela (Leningrad)* **14**, 3673 (1972) [*Sov. Phys.—Solid State* **14**, 3075 (1973)].